PROPOSED TRNSYS MODEL FOR STORAGE TANK WITH ENCAPSULATED PHASE CHANGE MATERIALS

Katherine D'Avignon[1], Michaël Kummert[1]
[1]Ecole Polytechnique, Montreal, Canada

ABSTRACT

Latent heat storage (LHS) using phase change materials (PCM) is a promising avenue to resolve the frequent timing mismatch between energy supply and demand. This paper deals with the modelling and simulation of a versatile thermal energy storage (TES) tank filled with encapsulated PCMs of rectangular geometry.

A simple model is developed and implemented as a TRNSYS component with the long-term goal of selecting optimal phase change temperature and testing control strategies for demand-side management and renewable energy applications. The model uses the enthalpy method and assumes phase change occurs over a small temperature range.

A comparison of model results to numerical results found in the literature indicates that it can predict the dynamic performance of this type of thermal energy storage tank with reasonable accuracy during loading and off-loading cycles. A simple example is used to demonstrate the use of the model in TRNSYS. Further work will aim to improve the model and validate it against experimental measurements.

INTRODUCTION

Some of the greatest scientific challenges of this century relate to our usage of energy; optimizing system energy use, reducing demand and developing renewable energy resources are prime examples. An important part of this issue is the constant mismatch between energy supply and demand. The dilemma is not the absence of energy per say but rather it is to find ways of supplying sufficient amounts, in a usable form, when and where it is required. Energy storage devices are one solution to this issue. They can reduce peak loads by deferring energy use, improve system performance by allowing them to work in their optimal range and provide backup power during an outage.

Amongst the batteries and flywheels, latent heat storage can address a particular clientele looking specifically for energy in the form of heat. As building heating and cooling, hot water production and refrigeration represented over 60% of the 20 quadrillion Btu consumed in US buildings in 2008 (U.S. Department of Energy, 2010), phase change materials have received much attention in the last decade. Their high-energy storage density and capacity to store and supply energy at nearly constant temperature are advantageous when compared to sensible heat storage systems.

Rectangular slab-like PCM encapsulation has been studied in numerous air-based applications. Dolado et al. (2006) developed four models to simulate the behaviour of slab-like PCM exposed to air flow and determined that a one-dimensional finite difference model with implicit formulation was sufficiently accurate to replicate experimental results. The paper also showed that considering conduction in the direction of heat transfer fluid (HTF) flow inside the PCM did not improve the model's agreement with experimental results. Halawa et al (2005) analysed melting and freezing of a LHS unit considering a varying PCM capsule wall temperature along the direction of HTF flow. To do this, they implemented local Nusselt number values calculated for constant temperature boundary conditions over the length of individual HTF control volumes but no experimental validations were made. Vakilaltojjar and Saman (2001) developed three computer models for the evaluation of a phase change storage system for air-conditioning where PCM slabs of different phase change temperatures are used in series. They tested various parameters to improve the storage performance and showed that the air-side heat transfer resistance dominates the overall heat transfer resistance.

The study of encapsulated PCM of rectangular geometry has been scarce for liquid HTF applications. Elsayed (2007) studied ice encapsulated in a horizontal slab and exposed to cyclic HTF temperatures. The author found that as the heat transfer efficiency is more affected by the HTF temperature than by the convection heat transfer coefficient, the mean HTF temperature can be used to determine the storage unit's response with sufficient precision. Liu et al. (2011b) produced a one-dimensional model for encapsulated PCM of rectangular geometry subjected to liquid HTF which showed reasonable agreement when compared to

experimental data. The model was later used in a parametric study which indicated that the inlet HTF temperature and flow rate have a significant impact on the melt duration and heat transfer rate (Liu et al., 2011a). Bony and Citherlet (2007) implemented a numerical model of PCM capsules in an existing TRNSYS type of a hot water tank, to reproduce the behaviour of a tank filled with encapsulated PCMs of various geometry, including rectangular capsules, though experimental tests were only made for cylindrical capsules. Puschnig et al (2005) also developed a TRNSYS model capable of representing water tanks filled with PCMs of various geometry as well as PCM slurry. Both models consider the tank to be vertical and as such stratification and natural convection are important components of the heat transfer occurring between the HTF and the PCM. Most other studies considered constant temperature boundary conditions (Costa et al., 1998, Silva et al., 2002, Lacroix, 2001, Hamdan and Elwerr, 1996) rather than convective heat transfer due to liquid flow.

This paper presents a simple model for horizontal storage tanks with encapsulated PCM of rectangular geometry. Unlike previous models for horizontal tanks, this model is to be used in full building simulations through use as a TRNSYS type. Emphasis is thus placed on computability and the accuracy of output HTF temperature on the time scale of typical building system response. The mathematical model developed is based on a variant of the so-called enthalpy method introduced by Voller (1990), as used by Bony and Citherlet (2007). Model results will be compared to numerical and experimental results found in the literature. Grid convergence and error estimation are discussed as well as model usefulness for system design.

MATHEMATICAL MODEL

The LHS unit studied is rectangular in shape and has adiabatic walls. It includes a number of flat slab-like PCM capsules laid-out in rows and columns with HTF flowing horizontally in the space between the PCM capsules.

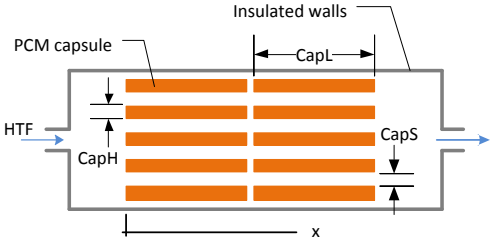

Figure 1: LHS unit with PCM capsules

In the development of a mathematical model for the LHS unit, the following assumptions are made:

- Effects of natural convection within the HTF and the liquid phase of the PCM are negligible;
- The PCM behaves as an ideal material (phenomena such as degradation or subcooling are not considered at this stage);
- Phase change occurs along a small temperature variation with no hysteresis between the freezing and melting processes;
- The PCM is homogeneous and isotropic with different properties for the liquid and solid phase;
- The PCM capsule's lateral faces are adiabatic, i.e., heat transfer occurs only through faces at y = 0 and y = CapH (see Figure 3);
- The conduction between two adjacent PCM control volumes (C.V.) is neglected. Only the energy transferred through the capsule wall by convection with the HTF is considered to affect the PCM C.V.

Based on these assumptions, a mathematical model is developed which uses subsequent energy balances over a small HTF control volume and the associated PCM control volume to establish the HTF output temperature from the LHS unit.

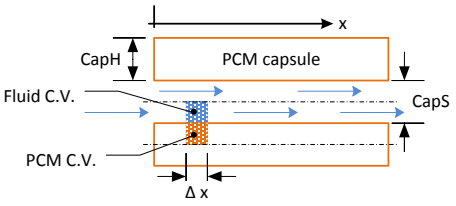

Figure 2: Model control volumes

Heat transfer fluid

The temperature of the HTF evolves as it flows between the PCM capsules and exchanges energy with the capsule wall. For each control volume considered, the energy balance results in equation [1]:

$$\frac{dC_f T}{dt} = \dot{m} c_{pf} (T_{in} - T_{out}) + h_f A_f (T_w - T_f) \qquad [1]$$

The term on the left represents the net rate of energy stored in the fluid control volume over a certain time step, with C_f being the fluid's heat capacity. Term $\dot{m}\, c_{pf} (T_{in}\text{-}T_{out})$ represents the net rate of energy transport into the control volume through advection, with $\dot{m}$ the HTF mass flow rate through the control volume and c_{pf} the HTF's specific heat capacity at a constant pressure. Term $h_f A_f (T_w\text{-}T_f)$ represents the net

rate of energy exchanged between the fluid and the PCM capsule wall through convection, with h_f the heat transfer coefficient and A_f the surface area of the convective exchange. The energy transferred depends on the difference between the capsule wall temperature, T_w, and fluid temperature, T_f, for the control volume considered.

Using backward time differentiation to solve for the net rate of energy stored in the HTF control volume:

$$\frac{dC_f T}{dt} = \frac{C_f\left(T_f - T_f^0\right)}{\Delta t} = \frac{\rho_f c_{pf} V_f \left(T_f - T_f^0\right)}{\Delta t} \quad [2]$$

With ρ_f the HTF density, c_{pf} the HTF's specific heat capacity at a constant pressure and V_f the volume of the control volume. The HTF temperature entering and leaving the control volume are considered as the time average values over the time step such that:

$$T_{in} - T_{out} = \frac{T_{f(i-1)} + T_{f(i-1)}^0}{2} - \frac{T_f + T_f^0}{2} \quad [3]$$

Values from the previous time step are indicated with superscript "0" while values from the upstream control volume are indicated with subscript "(i-1)". Similarly, time average values of the PCM capsule wall temperature and HTF temperature are used so:

$$T_w - T_f = \frac{T_w + T_w^0}{2} - \frac{T_f + T_f^0}{2} \quad [4]$$

Combining equations 1, 2, 3 and 4, the temperature of the HTF control volume becomes [5]:

$$T_f = \frac{(a - b - c)T_f^0 + c\left(T_{f(i-1)}^0 + T_{f(i-1)}\right) + b(T_w^0 + T_w)}{a + b + c} \quad [5]$$

Where $a = \rho_f c_{pf} V/\Delta t$, $b = h_f A_f/2$ and $c = \dot{m} c_{pf}/2$.

Heat transfer to PCM capsule

In this model, the thermal inertia of the capsule wall is neglected and so all the energy transferred to the capsule wall from the HTF, q_{conv}, is simultaneously transferred to the associated PCM control volume through conduction, q_{cond}. Both energy fluxes are established through equations 6 and 7:

$$q_{conv} = h_f A_f \left\{\frac{{T_f}^0 + T_f}{2} - \frac{{T_w}^0 + T_w}{2}\right\} \quad [6]$$

$$q_{cond} = \frac{k_{pcm} A_{pcm}}{\Delta y}\left\{\frac{{T_{pcm}}^0 + T_{pcm}}{2} - \frac{{T_w}^0 + T_w}{2}\right\} \quad [7]$$

Where k_{pcm} is the PCM conductivity, A_{pcm} is the surface area of the conductive exchange and Δy is the distance over which occurs the conduction; in this case, the distance between the PCM capsule wall and the center of the PCM capsule. This equality between equations 6 and 7 allows the formulation of an equation to evaluate the capsule wall temperature [8]:

$$T_w = \frac{b\left(T_f^0 + T_f\right) - (b + d)T_w^0 + d\left(T_{pcm} + T_{pcm}^0\right)}{b + d} \quad [8]$$

Where $b = h_f A_f/2$ and $d = k_{pcm} A_{pcm}/2\Delta y$.

Phase change

During phase transition, both the liquid and solid phases of the PCM are present and are separated by an interface that is constantly shifting. On each side of this boundary, the properties of the material can be quite different. Predicting the behaviour of a PCM during phase change is thus categorized as a moving boundary problem. Multiple numerical methods have been developed to solve this type of problem (Bansal and Buddhi, 1992). The method used here is a variant of the so-called enthalpy method introduced by Voller (1990) which does not require the explicit treatment of conditions at the phase change interface, so the boundary position need not be traced throughout the domain. In fact, as this method uses the same governing equation for the two phases, any sharp discontinuities at the phase change interface are avoided. This method has been used successfully by other authors to simulate the behaviour of PCM capsules (Bony and Citherlet, 2007, Puschnig et al., 2005). However, it presents other drawbacks; namely, the temperature field is not calculated explicitly but through enthalpy-temperature correlations. Though this correlation is not always supplied by PCM manufacturers, it can be determined experimentally through the temperature-history method as modified by Marín et al (2003).

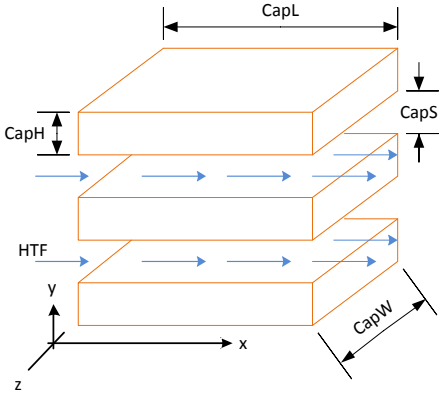

Figure 3: PCM capsule characteristic dimensions

Thus, following the determination of the HTF and capsule wall temperatures, the change in the PCM state is then determined by calculating the change in enthalpy with equation 9:

$$H = H^0 + q_{conv}\Delta t \quad [9]$$

Where H is the current PCM enthalpy and H^0 is the PCM enthalpy for the same node from the last time step. The new PCM control volume temperature is then

found through spline interpolation of the specific enthalpy-temperature curve.

PCM properties

Though the PCM thermal conductivity, k_{pcm}, is considered constant within one phase, it will vary during the simulation according to the PCM state. During phase change, its value is neither that of the solid, k_s, nor that of the liquid state, k_l, rather it is determined through a linear interpolation between the liquid and solid state values according to the enthalpy of each PCM control volume, H:

$$k_{pcm} = k_s + \frac{(H - H_{sm}) * (k_l - k_s)}{H_{sf} - H_{sm}} \quad [10]$$

Thus, a reference enthalpy is calculated for the start of the freezing process, H_{sf}, and the start of the melting process, H_{sm}. These reference enthalpies are located at the limit of the beginning of the phase change and represent respectively a liquid fraction, l_f, of 1 and 0. They are determined through linear interpolation from the specific enthalpy-temperature curve using the temperature at the start of the freezing process, T_{sf}, and that at the start of the melting process, T_{ef}, supplied by the user. The PCM liquid fraction during phase change is determined through the same method.

Heat transfer coefficient

The geometry of the rectangular PCM capsules is suitable to using the general case of forced convection between parallel plates in determining the heat transfer coefficient. Though this model is based on control volumes encompassing only half HTF flow passage height, the Nusselt number is calculated for the full passage height. As the PCM temperature is nearly constant while phase change is occurring, constant temperature boundary conditions at applied at each plate. Normal operating conditions will lead to laminar flow in the space between capsules which will be considered hydro-dynamically developed. As such, the following correlation, introduced by Shah and London (1978), can be used over the length of the PCM capsules to determine the flow length average Nusselt number, $Nu_{m,T}$:

$$Nu_{m,T} = \begin{cases} 1.849(x^*)^{-1/3} & x^* \leq 0.0005 \\ 1.849(x^*)^{-1/3} + 0.6 & 0.0005 < x^* \leq 0.006 \\ 7.541 + 0.0235/x^* & 0.006 < x^* \end{cases} \quad [11]$$

Where x* is the dimensionless distance in the direction of HTF flow which is determined by $x^* = x/(D_h PrRe)$ where D_h is the hydraulic diameter, Pr is the HTF's Prandtl's number and Re is Reynold's number. The heat transfer coefficient, h_f, is then calculated from the Nusselt number through the relation: $h_f = Nu^* k_f / D_h$ where k_f is the HTF thermal conductivity.

COMPUTER MODEL

A computer model based upon this mathematical paradigm was first developed and tuned in Matlab and later incorporated into TRNSYS.

Initial conditions

For the first simulation time step, the entire TES tank is supposed to be at the same temperature, T_{ini}, which is either greater than T_{sf} or lesser than T_{sm} so that the PCM is either completely solid or completely liquid. All PCM and HTF properties are then initialized based upon this temperature. For all other time steps, the hypothesis used initializes all properties based upon the temperature from the past time step.

Convergence criteria

Convergence toward a stable solution is verified for each control volume, at every time step, through the comparison of the different TES tank temperatures at the current and past time steps. The absolute change in temperature between two iterations must be less than 10^{-3} °C for the PCM capsule wall temperature, PCM temperature and HTF temperature for convergence to be reached. This is expressed through equation [12]:

$$\text{If } \begin{cases} |T_w^0 - T_w| \leq 10^{-3} \\ \text{and } |T_f^0 - T_f| \leq 10^{-3} \\ \text{and } |T_{pcm}^0 - T_{pcm}| \leq 10^{-3} \end{cases} \text{ then convergence [12]}$$

VERIFICATION OF CALCULATIONS

In order to ascertain the validity of the model for the desired application, the calculations were verified through a study of convergence where the numerical model was used with varying space and time increments, Δx and Δt. The input temperature used was a step function, initially cooling the PCM with HTF injected at 30°C for 12 hours and later heating the PCM with a HTF at 62°C for another 12 hours. Water was used as the HTF with a constant mass flow rate of 0.055 kg/s for the length of the simulation. The PCM capsules were 0.5m x 0.25m x 0.038m with a spacing of 0.007m. The TES tank contained 3 rows of 3 capsules in length, each row being 8 capsules high. The properties of the PCM used are listed in Table 1.

Table 1: PCM properties

PROPERTIES	LIQUID	SOLID
Specific heat [J/kg-°C]	4226	1762
Density [kg/m^3]	1000	1000
Thermal conductivity [W/m-°C]	0.556	2.22
Latent heat of fusion [J/kg]	338 000	
Melting temperature [°C]	46.1	
Freezing temperature [°C]	45.9	
Initial temperature [°C]	50.0	

A constant refinement ratio of 2 was used for Δx with a conservative time increment of Δt = 1s. The HTF output temperature profiles of each space increment evaluated are shown on Figure 4. A clear oscillation of the output temperature can be seen for Δx = 100mm during the freezing process but is present, to a lesser extent, for all grid spacings. These disruptions occur only during the freezing process, culminating soon after the 12hr mark when the PCM abruptly changes from cooling to heating.

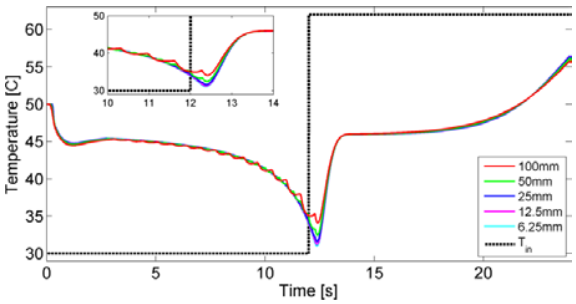

Figure 4: Verification of space increment

Narrowing in on space increments of less than 25 mm, a grid convergence study was done with a constant refinement ratio of 1.25 resulting in Δx of 23.4375 mm, 18.75 mm, 15 mm and 12 mm. A posteriori error estimates were performed for the simulation results through the use of the Richardson extrapolation as used by Roache (1997). Only part of the heating phase was used in this analysis so as to eliminate the impact of the oscillating results from the grid analysis. The error estimates were calculated for every space increment, at every time step from t = 12.5hrs to t = 21hrs. Calculation results showed to be in the asymptotic region for the time interval studied. The estimated maximum error over the simulation for each grid spacing is displayed in Table 2.

Table 2: Error estimates and GCI for various Δx

ΔX	MAXIMUM ERROR	MEAN GCI
23.4375 mm	0.617 °C	21.1%
18.75 mm	0.493 °C	16.9%
15 mm	0.391 °C	13.5%
12 mm	0.311 °C	10.8%

The grid convergence index (GCI) as developed by Roache (1994) was also calculated for each grid increment and its mean value over the part of the heating phase studied is reported in Table 2. The values stated fall between those cited by Roache (1994) for first-order methods with refinement indexes of 1.1 and 1.5. From these results, a space increment of Δx = 20mm is selected for all further calculations so as to compromise between calculation accuracy and computing time.

A similar analysis is performed for varying time increments using a constant refinement ratio of 2 and keeping the space increment constant at Δx = 20mm. The HTF output temperature profiles of each space increment evaluated are shown on Figure 5. The slight variations in HTF output temperature (0.1°C maximum) between the different time increments are negligible and no oscillation of T_{out} are visible during the freezing process.

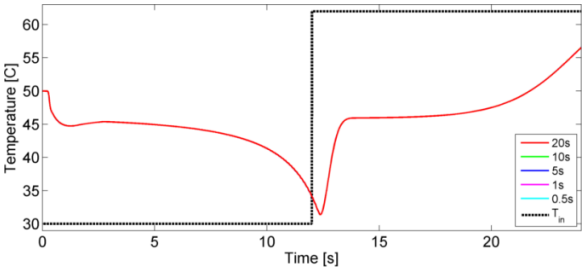

Figure 5: Verification of time increment

The a posteriori error estimates and grid convergence indexes are calculated and their mean values over the whole simulation are illustrated in Table 3. The errors reported are negligible in the context of most real HVAC applications and so it is deduced that the various time increments evaluated are acceptable when combined with a space increment of Δx = 20mm. A time increment of Δt = 1 s is selected for all further calculations.

Table 3: Error estimates and GCI for various Δt

ΔT	MEAN ESTIMATED ERROR	MEAN GCI
20 s	0.0096 °C	2.88%
10 s	0.0079 °C	2.37%
5 s	0.0087 °C	2.60%
1 s	0.0082 °C	2.46%
0.5 s	0.0051 °C	1.52%

Comparison to experimental results

In order to further verify the developed model, a comparison is made against experimental results from the literature. In this case, results for Test 1 from the work of Liu et al. (2011b) are used. Our original intent was to perform a more thorough model validation using the published experimental data, but the paragraphs below will show that there are many uncertainties on some of the input parameters presented (or omitted) in the paper. Unfortunately the authors did not respond to our queries for clarifications. The comparison is still presented in this paper, as it represents a different test case from the systematic tests presented above.

Most input parameters for the present model can be found in the reference article. The PCM thermal conductivity for the liquid and solid phase are those from Table 1, as they are not mentioned in the article. The specific enthalpy-temperature curve is built from the latent heat of fusion, specific heat and freezing temperature data from the reference article, assuming T_{sf} = -26.6 °C and T_{sm} = -26.8 °C as the test only includes a PCM melting process. In order to replicate the HTF viscosity and crystallization point mentioned in the reference article, water with an ethylene glycol content of 60% is used as HTF.

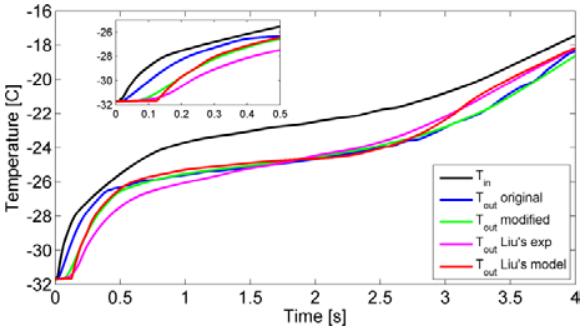

Figure 6: Comparison of Tout from the present model to data from Liu et al. (2011b)

Initial results using 19 parallel capsules result in a longer phase change period than displayed by both experimental and model results from the reference article. Using 10 parallel capsules, model results show to be in the same range as those from the work cited and fit more closely with the 136.8 kg mass of PCM referred to in the article. A value of 10 capsules is used for further calculations. All other PCM and HTF properties as well as input parameters are the same as those of the work cited.

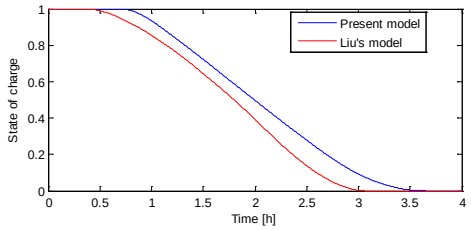

Figure 7: State of charge predicted by both models

Results from the comparison of HTF output temperature, T_{out}, from the various sources are presented in Figure 6 and the state of charge of the TES tank predicted by both models is presented in Figure 7. The model presents a similar profile to data from the work of Liu et al. A noticeable discrepancy occurs at the beginning of the simulation (t < 0.5hrs), where T_{out} is much warmer for the present model than for both the experimental and reference model results. This would appear to indicate more energy from the HTF is being stored somewhere in the TES tank than for the present model. As shown in Figure 7, the phase change does not begin for either the present or the reference model until after t = 0.5hr. The sensible heating of the PCM capsules is insufficient to account for all the HTF energy being stored in the LHS unit. An additional volume of HTF present elsewhere in the LHS unit than strictly in the spaces between the PCM capsules would account for the extra energy being stored.

The model is modified to account for an additional volume of HTF present at both ends of the LHS unit. These volumes of HTF would be present in most experimental set-ups as entry and exit lengths would be required to allow proper flow of HTF across all PCM capsules. Adding an entry and exit length of 0.5 m and reducing the liquid phase thermal conductivity to 0.1 W/m-°C, the model produces a delay before T_{out} increases for t < 0.5hrs. The modified parameters lead to better fit to the experimental and model data from Liu et al.'s work (Figure 6).

APPLICATION IN TRNSYS SIMULATION

The developed model was implemented in a simple simulation to illustrate its potential in system-level analyses. The test case consists of a simple solar thermal system for space heating, and the PCM tank is compared to a reference case with stratified water storage. System configurations are shown in Figure 8.

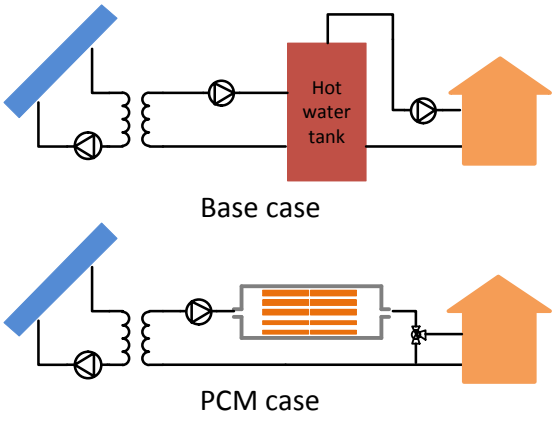

Figure 8: Solar storage example

The simulation is run for a periodic day to illustrate the differences in sizing and temperature levels between the two storage options. Ambient conditions are taken for a sunny and cold February day (temperature between -15 °C and 0 °C, clear sky radiation). The heating load peaks at 1 kW and its profile is shown in Figure 9.

The simulation uses standard TRNSYS components except for the PCM tank. The water storage tank is modeled using the standard component known as Type 4. The reference case is sized to meet the entire heat demand without auxiliary heating and it uses a storage volume to collector area ratio of 100 L/m². The smallest system that is capable of providing 45 °C (selected as the arbitrary setpoint) all the time consists of 4.7 m² of solar collectors (standard flat-plate) and 470 L of water storage.

A comparison is made with a system where the water tank is replaced with a PCM tank containing capsules with a 46 °C phase change temperature (see Table 1 for detailed properties). The PCM configuration does not benefit from stratification and a slightly larger collector area (5 m²) is required to meet the load without an auxiliary heater. The required PCM tank includes 76 L of phase change material.

The design conditions impose that the daily collected solar heat is equal to the the daily heating load. This can be seen in Figure 9, but there is a small difference between the two systems: the water tank is stratified, which provides a better collector efficiency at the peak of solar collection, while the PCM tank provides an almost constant supply temperature to the collectors, which is beneficial when the storage is at the peak of its charging cycle. The heating supply temperature just reaches 45 °C at the lowest point, again by design in this simple example. Figure 9 shows that the heating supply temperature (or tank outlet temperature) has a very different profile in both cases: the water tank temperature more or less follows the imbalance between supply and demand, while the PCM tank outlet temperature remains approximately constant until the state of charge (liquid fraction of the PCM) reaches zero or one, when the temperature starts drifting much faster.

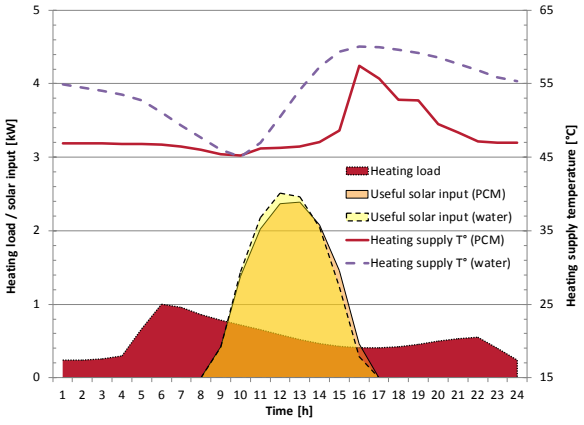

Figure 9: Comparison between water and PCM tanks

Indicative running times on a modern laptop computer are 13 min for 365 repetitions of the daily cycle with the PCM tank, versus 6 min for the reference case using Type 4 with 3 thermal nodes. All simulations use a 30-s time step.

CONCLUSIONS

This paper presented a one-dimensional model for horizontal storage tanks with encapsulated PCM of rectangular geometry, which was developed and implemented successfully in TRNSYS. A grid convergence study allowed to select the appropriate space and time increments for the model. The independence of model outputs from time increment used promises great flexibility for future implementation in a complete building simulation. The model's calculation results were compared to experimental data from the literature. With the addition of entry and exit lengths, the model shows reasonable agreement with experimental data from the literature both in terms of the HTF output temperature and the heat transfer rate. Although many uncertainties persist upon the input parameters used in the reference article, the model demonstrates its potential in replicating real PCM LHS unit behavior for building system simulations. Future work will include thorough experimental tests to properly validate the model.

REFERENCES

BANSAL, N. K. & BUDDHI, D. 1992. An Analytical Study of a Latent Heat Storage System in a Cylinder. Journal of Energy Conversion and Management, 33, 235-242.

BONY, J. & CITHERLET, S. 2007. Numerical Model and Experimental Validation of Heat Storage with Phase Change Materials. Journal of Energy and Buildings, 39, 1065-1072.

COSTA, M., BUDDHI, D. & OLIVA, A. 1998. Numerical Simulation of a Latent Heat Thermal Energy Storage System with Enhanced Heat Conduction. Journal of Energy Conversion and Management, 39, 319-330.

DOLADO, P., LÁZARO, A., ZALBA, B. & MARIN, J. M. Numerical Simulation of the Thermal Behaviour of an Energy Storage Unit with Phase Change Materials for Air Conditioning Applications Between 17°C and 40°C. ECOSTOCK 10th international conference on thermal energy storage, 2006 The Richard Stockton College of New Jersey.

ELSAYED, A. O. 2007. Numerical Study of Ice Melting Inside Rectangular Capsule under Cyclic Temperature of Heat Transfer Fluid. Energy Conversion and Management, 48, 124-130.

HALAWA, E., BRUNO, F. & SAMAN, W. 2005. Numerical analysis of a PCM thermal storage system with varying wall temperature. Energy Conversion and Management, 46, 2592-2604.

HAMDAN, M. A. & ELWERR, F. A. 1996. Thermal Energy Storage Using Phase Change Material. Journal of Solar Energy, 56, 183-189.

LACROIX, M. 2001. Contact melting of a phase change material inside a heated parallelepedic capsule. Journal of Energy Conversion and Management, 42, 35-47.

LIU, M., BRUNO, F. & SAMAN, W. 2011a. Thermal performance analysis of a flat slab phase change thermal storage unit with liquid-based heat transfer fluid for cooling applications. Journal of Solar Energy, 85, 3017-3027.

LIU, M., SAMAN, W. & BRUNO, F. 2011b. Validation of a Mathematical Model for Encapsulated Phase Change Material Flat Slabs for Cooling Applications. Journal of Applied Thermal Engineering, 31, 2340-2347.

MARIN, J. M., ZALBA, B., CABEZA, L. F. & MEHLING, H. 2003. Determination of enthalpy-temperature curves of phase change materials with the temperature-history method: improvement to temperature dependent properties. Journal of Measurement Science and Technology, 14.

PUSCHNIG, P., HEINZ, A. & STEICHER, W. 2005. TRNSYS simulation model for an energy storage for PCM slurries and/or PCM modules. Second Conference on Phase Change Material & Slurry: Scientific Conference & Business Forum. Yverdon-les-Bains, Switzerland.

ROACHE, P. J. 1994. Perspective: A Method for Uniform Reporting of Grid Refinement Studies. Journal of Fluids Engineering, 116, 405-413.

ROACHE, P. J. 1997. Quantification of uncertainty in computational fluid dynamics. Annual Review of Fluid Mechanics, 29, 123-160.

SHAH, R. K. & LONDON, A. L. 1978. Laminar flow forced convection in ducts, New York, Academic Press.

SILVA, P. D., GONÇALVES, L. C. & PIRES, L. 2002. Transient Behaviour of a Latent-Heat Thermal Energy Store: Numerical and Experimental Studies. Journal of Applied Energy, 73, 83-98.

U.S. DEPARTMENT OF ENERGY, E. E. A. R. E. 2010. 2010 Buildings Energy Data Book. In: U.S. DEPARTMENT OF ENERGY, E. E. A. R. E. (ed.). Pacific Northwest National Laboratory.

VAKILALTOJJAR, S. M. & SAMAN, W. 2001. Analysis and modelling of a phase change storage system for air conditioning applications. Journal of Applied Thermal Engineering, 21, 249-263.

VOLLER, V. R. 1990. Fast Implicit Finite-Difference Method for the Analysis of Phase Change Problems. Journal of Numerical Heat Transfer, 17 (part B), 155-169.

NOMENCLATURE

A_f: surface area of the convective exchange [m^2]
A_{pcm}: surface area of the conductive exchange [m^2]
C: heat capacity [J/K]
c_{pf}: HTF constant pressure specific heat [J/kg*K]
D_h: hydraulic diameter [m]
H: enthalpy [J]
H_{sf}: enthalpy at the start of the freezing process [J]
H_{sm}: enthalpy at the start of the melting process [J]
h_f: HTF heat transfer coefficient [W/K-m^2]
k_f: HTF thermal conductivity [W/m-K]
k_l: PCM liquid state thermal conductivity [W/m-K]
k_{pcm}: PCM thermal conductivity [W/m-K]
k_s: PCM solid state thermal conductivity [W/m-K]
l_f: liquid fraction [-]
M_{pcm}: mass of one PCM control volume [kg]
$\dot{m}$: HTF mass flow rate [kg/s]
$Nu_{m,T}$: flow length average Nusselt number [-]
Pr: Prandtl's number [-]
q_{conv}: energy transferred to the capsule wall from the HTF [J/kg]
q_{cond}: energy transferred to the PCM control volume through conduction [J/kg]
Re: Reynolds number [-]
T_{ini} : initial TES tank temperature [K]
T_f : HTF temperature [K]
T_w : PCM capsule wall temperature [K]
T_{pcm} : PCM temperature [K]
T_{sf}: PCM temperature at the beginning of the freezing process [K]
T_{sm}: PCM temperature at the beginning of the melting process [K]
V_f: volume of the HTF control volume [m^3]
x*: dimensionless distance [-]

Greek symbols

ρ_f: HTF density, kg/m^3
Δt: simulation time step, s
Δy: distance of conduction heat exchange, m

Subscript

i-1: values from the upstream control volume
ini: initial
f: heat transfer fluid
l: liquid state
pcm: phase change material
s: solid state
sf: start of freezing process
sm: start of melting process
w: PCM capsule wall

Superscript

0: values from the previous time step